

Alma Mater Studiorum Università di Bologna
Archivio istituzionale della ricerca

Ciprofloxacin carrier systems based on hectorite/halloysite hybrid hydrogels for potential wound healing applications

This is the final peer-reviewed author's accepted manuscript (postprint) of the following publication:

Published Version:

Massaro, M., Borrego-Sánchez, A., Sánchez-Espejo, R., Viseras Iborra, C., Cavallaro, G., García-Villén, F., et al. (2021). Ciprofloxacin carrier systems based on hectorite/halloysite hybrid hydrogels for potential wound healing applications. *APPLIED CLAY SCIENCE*, Volume 215, 1-12 [10.1016/j.clay.2021.106310].

Availability:

This version is available at: <https://hdl.handle.net/11585/878147> since: 2022-03-11

Published:

DOI: <http://doi.org/10.1016/j.clay.2021.106310>

Terms of use:

Some rights reserved. The terms and conditions for the reuse of this version of the manuscript are specified in the publishing policy. For all terms of use and more information see the publisher's website.

This item was downloaded from IRIS Università di Bologna (<https://cris.unibo.it/>).
When citing, please refer to the published version.

(Article begins on next page)

Ciprofloxacin carrier systems based on hectorite/halloysite hybrid hydrogels for potential wound healing applications

Marina Massaro,^{†,a} Ana Borrego-Sánchez,^{†,b,c} Rita Sánchez-Espejo,^d César Viseras Iborra,^{*c,d}
Giuseppe Cavallaro,^{e,f} Fátima García-Villén,^c Susanna Guernelli,^g Giuseppe Lazzara,^{e,f} Dalila
Miele,^h C. Ignacio Sainz-Díaz,^d Giuseppina Sandri^h and Serena Riela^{*a}

^a Department of Biological, Chemical and Pharmaceutical Sciences and Technologies, University
of Palermo Viale delle Scienze, Ed. 17 90128, Palermo, Italy, E-mail: serena.riela@unipa.it.

^b Center for Human Technologies, Italian Institute of Technology, Via Enrico Melen 83, 16152
Genoa, Italy.

^c Department of Pharmacy and Pharmaceutical Technology, Faculty of Pharmacy. University of
Granada, Campus of Cartuja, 18071 s/n, Granada, Spain. E-mail: cviseras@ugr.es.

^d Andalusian Institute of Earth Sciences, CSIC-UGR. Avenida de las Palmeras 4, 18100 Armilla,
Granada, Spain.

^e Dipartimento di Fisica e Chimica, Università di Palermo, Viale delle Scienze, 90128 Palermo,
Italy.

^f Consorzio Interuniversitario Nazionale per la Scienza e Tecnologia dei Materiali, INSTM, I-
50121 Firenze, Italy.

^g Dipartimento di Chimica “Giacomo Ciamician”, Via S. Giacomo 11, Bologna, Italy.

^h Department of Drug Sciences, University of Pavia, viale Taramelli 12, 27100, Pavia, Italy.

[†] Contributed equally

KEYWORDS. Clay minerals, halloysite, hectorite, hybrid hydrogel, wound healing, drug carrier

ABSTRACT. The design of multifunctional nanomaterials which can help the healing processes of skin, preventing the bacterial infections, is crucial for the development of suitable therapy for the treatment of chronic lesions. The use of clay minerals in wound healing applications is well documented since the prehistoric period and offers several advantages due to their intrinsic properties.

Herein, we report the development of ciprofloxacin carrier systems based on hectorite/halloysite (Ht/Hal) hybrid hydrogels for potential wound healing applications. To achieve this objective firstly the ciprofloxacin molecules were loaded onto Hal by a supramolecular and covalent approach. The so obtained fillers were thoroughly investigated by several techniques and at molecular level by means of quantum mechanics calculations along with empirical interatomic potentials. Afterwards the modified Hal were used as filler for Ht hydrogels. The introduction of modified Hal, in hectorite hydrogel, helps the gel formation with an improvement of the rheological properties. The *in vitro* kinetic release from both the fillers and from the hybrid hydrogels was studied both at skin's pH (5.4) and under neutral conditions (pH 7.4); in addition, the factors controlling the ciprofloxacin release process were determined and discussed. Finally, the *in vitro* biocompatibility of the Hal fillers was evaluated by means of cytotoxic assays and laser scanning confocal microscopy on normal human dermal fibroblasts.

INTRODUCTION. Skin, the biggest organ, represents the natural barrier between the body and the outside world protecting it from the invasion of external microorganisms. When a trauma occurs, the skin tissue is damaged, and it becomes exposed to the external environment. Acute wounds generally heal within few weeks, but if the healing process is somehow impaired

46 chronic wounds occur with a healing time greater than 12 weeks. A delay in wound healing
47 could pose serious and life-threatening medical conditions which could lead to amputation.
48 Bacterial infection is one of the most serious issues that can impair healing (Hu and Xu,
49 2020; Liang et al., 2019).

50 In the last years, the use of clay minerals for application in biomedical field has proven to
51 be advantageous, mostly in tissue engineering since they can enhance cell attachment,
52 proliferation and differentiation (Dawson and Oreffo, 2013; Naumenko et al., 2016), acting
53 as antimicrobials as well (Williams et al., 2011).

54 Hydrogels formed by fibrous clay, have attracted considerable attention since they can
55 promote wound healing process and offer several advantages for topical drug delivery such
56 as prolonged sustained release as well as ease of administration (Sharifzadeh et al., 2020).
57 Furthermore, they are biocompatible and show high swelling capacity, that are crucial for
58 the diffusion of active molecules into the target site (Kevadiya et al., 2014). Hectorite (Ht)
59 is a clay of smectite groups which possesses the ability to form stable hydrogels in aqueous
60 regime. Biocompatibility studies have shown that its hydrogels possess potential wound
61 healing activity (García-Villén et al., 2021).

62 Fluoroquinolone compounds such as ciprofloxacin (Cipro), are widely used as antibiotics
63 to treat skin infections since they are among the most used broad-spectrum antibiotics
64 (Campoli-Richards et al., 1988).

65 However, ciprofloxacin suffers from some inconveniences which limit its clinical use, *i*) Cipro
66 is insoluble in physiological conditions (Korzeniowska et al., 2020) and *ii*) it presents poor
67 permeability across cell membranes (Breda et al., 2009). Unfortunately, there are some
68 limitations in the use of hectorite as carrier for the hydrophobic Cipro (Massaro et al.,

2021b), so the introduction of a filler in the hectorite hydrogel, that acts as a carrier, could be advantageous. Recently, the combination, both by a supramolecular and a covalent approach, of two different clay minerals with complementary properties has been investigated. It was found that the obtained hybrid materials showed improved physico-chemical and biological properties compared to pristine components which make them attractive for biological purposes (Massaro et al., 2021b).

Halloysite nanotubes (Hal) are an aluminosilicate clay with a predominantly hollow tubular structure and chemically similar to the platy kaolinite ($\text{Al}_2\text{Si}_2\text{O}_5(\text{OH})_4 \cdot n\text{H}_2\text{O}$). Generally, the length of the tubes is in the range of 0.2–1.5 μm , while their inner and outer diameters are in the ranges of 10–30 nm and 40–70 nm, respectively (Liu et al., 2014). Hal, naturally occurring in huge quantities at low cost, show excellent bio-(Fakhrullina et al., 2015; Kryuchkova et al., 2016; Rozhina et al., 2021; Rozhina et al., 2020) and ecocompatibility (Bellani et al., 2016). Halloysite is positively charged in the inner lumen, which consists mostly of aluminum hydroxide, whereas the external surface, which is silicon dioxide, is negatively charged. However, the charge properties of Hal surfaces are strictly dependent from the pH depending on the protonation/deprotonation equilibria of the surface groups (Bretti et al., 2016). The different surface chemistry allows the selective functionalization at the inner and/or outer side making possible the synthesis of several nanomaterials with hierarchical nanostructure (Massaro et al., 2020b; Peixoto et al., 2021; Stavitskaya et al., 2018). Hal are widely used as enzyme immobilization (Tully et al., 2016), catalysts (Lin et al., 2020; Massaro et al., 2020a; Stavitskaya et al., 2020), environmental remediation (Massaro et al., 2016; Salaa et al., 2020), drug carriers (Massaro et al., 2019b; Massaro et al., 2020c) and delivery systems (Alfieri et al., 2022) and so on (Borrego-Sánchez et al.,

2018; Riela et al., 2021; Santos et al., 2019). Most importantly, Hal are able to penetrate the cellular membrane surrounding the cell nuclei (Gorbachevskii et al., 2021; Lvov et al., 2014). In addition, it has been proved that the modification of the tubes surfaces makes hybrid nanomaterials that penetrate the nucleus membrane, as well (Massaro et al., 2019a). Herein, we report the development of ciprofloxacin carrier systems based on Ht/Hal hybrid hydrogels for potential wound healing applications. Firstly, we studied the ciprofloxacin loading both supramolecular and covalently onto Hal. The fillers obtained were thoroughly characterized both from an experimental point of view and at molecular level by means of quantum mechanics calculations along with empirical interatomic potentials. Then, we explored the possibility of obtaining Ht hydrogels in the presence of modified Hal filler loaded with ciprofloxacin. The mechanical properties of the hydrogels obtained were examined by rheology measurements. The *in vitro* kinetic release from both the fillers and from the hybrid hydrogels was studied both at skin's pH (5.4) and under neutral conditions (pH 7.4); in addition, the factors controlling the ciprofloxacin release process were determined and discussed. Finally, the biocompatibility of the halloysite systems was also evaluated by means of cytotoxic assays and laser scanning confocal microscopy on normal human dermal fibroblasts.

2. MATERIALS AND METHODS.

All chemicals were obtained from Sigma-Aldrich and used as received. Hal-NH₂ was prepared as reported elsewhere.(Massaro et al., 2018b) FT-IR spectra (KBr) were acquired with an Agilent Technologies Cary 630 FT-IR spectrometer. The morphology of the nanomaterials was studied using an ESEM FEI QUANTA 200F microscope with EDX probe. The measurement was carried out in high-vacuum mode ($<6 \times 10^{-4}$ Pa). Before each experiment, the sample was coated with

gold in argon (60 s) by means of an Edwards Sputter Coater S150A to avoid charging under an electron beam. Differential scanning calorimetry (DSC) analyses were performed (Mettler Toledo, Columbus, OH, USA) using aluminum crucibles, a 30–400°C temperature range, at a heating rate of 10°C min⁻¹. All the analyses were performed in atmospheric air. X-ray powder diffraction (XRPD) analysis was carried out using a diffractometer (X'Pert Pro model, Malven Panalytical) equipped with a solid-state detector (X'Celerator) and a spinning sample holder. The diffractogram patterns were recorded using random oriented mounts with CuK α radiation, operating at 45 kV and 40 mA, in the range 4–60 °2 θ . Thermogravimetric (TG) analyses were carried out through a Q5000 IR apparatus (TA Instruments) under nitrogen atmosphere (gas flows of 25 and 10 cm³ min⁻¹ were employed for the sample and the balance, respectively). The experiments were carried out by heating the sample (ca. 5 mg) to 800°C. The heating rate was 20°C min⁻¹. The rheology measurements were recorded at room temperature on an DHR2 (TA Instruments) oscillatory rheometer using a parallel–plate (20 mm) tool; the sample was placed between the shearing plates of the rheometer. The rheological properties, such as strain sweep and frequency sweep, were recorded three times on three different aliquots of gels. The strain sweeps were performed at an angular frequency of 1 rad s⁻¹ and the frequency sweeps were performed at strains of 1%.

2.1. Loading of ciprofloxacin into Hal lumen (Hal/Cipro)

To a dispersion of Hal in MeOH (5 mL), 1 mL of a solution 10⁻² M of ciprofloxacin in HCl 0.1 N was added. The suspension was sonicated for 5 min, at an ultrasound power of 200 W and at 25°C and then was evacuated for 3 cycles. The suspension was left under stirring for 18 h at room temperature. After this time, the powder was washed with water and then dried at 60 °C.

2.2. Covalent grafting of Cipro onto Hal (Hal-Cipro)

Ciprofloxacin (50 mg, 0.15 mmol) was suspended in CH_2Cl_2 (10 mL), and N,N-dicyclohexylcarbodiimide (DCC) (35 mg, 0.15 mmol) was added. The suspension was stirred under an argon atmosphere at room temperature for 10 min. Then, Hal-NH_2 (100 mg) was quickly added. The mixture was stirred for 48 h. Then, the solvent was removed by filtration; the powder was then rinsed successively with H_2O and CH_2Cl_2 and finally dried at 80°C under vacuum.

2.3. Preparation of Ht hydrogels.

Pure gels were prepared by weighing into a screw-capped sample vial (diameter 2.5 cm) the amount of hectorite (100 mg) and solvent (~ 1 g). The mixture was first dispersed for 5 minutes with ultrasound irradiation and left at room temperature until a gel was obtained.

2.4. Preparation of Ht hybrid hydrogels.

Hybrid hydrogels were prepared by weighing into a screw-capped sample vial (diameter 2.5 cm) the amount of Ht (100 mg), modified Hal (5 mg) or Cipro (5 mg) and solvent (~ 1 g). The mixture was first dispersed for 5 minutes with ultrasound irradiation and subsequently left at room temperature until a gel was obtained.

2.5. Models

The adsorption complex models were created from the atomic coordinates of a slice of a halloysite nanotube from previous work (Guimarães et al., 2010) with the stoichiometry $\text{Al}_2\text{Si}_2\text{O}_5(\text{OH})_4$. Periodic boundary conditions of this nanotube were used to generate a periodical crystal structure, and the cell parameters of the structure was described previously (Borrego-Sánchez et al., 2017; Carazo et al., 2017). The unit cell of the nanotube of halloysite has an internal layer of aluminium hydroxide octahedral, with an internal diameter of 27 \AA , joined to an external layer of silicon oxide tetrahedra. This structure is a great model to reproduce the interactions at molecular level of the adsorption process. The unit cell of halloysite has the formula $\text{Al}_{76}\text{Si}_{76}\text{O}_{190}(\text{OH})_{152}$ with 646 atoms.

To carry out the adsorption of ciprofloxacin drug, a $1 \times 1 \times 2$ supercell of halloysite was generated with the formula $\text{Al}_{152}\text{Si}_{152}\text{O}_{380}(\text{OH})_{304}$ and with 1292 atoms. The ciprofloxacin drug was taken from crystallographic data (Turel et al., 1997). A molecule was extracted from the crystal to study its adsorption in the halloysite $1 \times 1 \times 4$ supercell.

2.6. Molecular modeling methodology

The optimization of the unit cell of halloysite nanotube structure was performed with quantum mechanical calculations by using Density Functional Theory (DFT) with CASTEP code of the Materials Studio package (BIOVIA, 2016). The functionals used were the Perdew–Burke–Ernzerhof (PBE) correlation exchange one in the generalized gradient approximation (GGA). On-the-fly generated (OTFG) ultrasoft pseudopotentials were used with Koelling-Harmon relativistic treatment (Vanderbilt, 1990), and the cut off energy of the calculation was 300 eV (BIOVIA, 2016). After the optimization of the halloysite unit cell, the $1 \times 1 \times 2$ supercell was created to study the adsorption of the drug. The ciprofloxacin molecule was optimized with the Compass Force Field (FF) by using the Forcite program that have provided good results in previous studies (Borrego-Sánchez et al., 2017; Borrego-Sánchez et al., 2016) (BIOVIA, 2016). For non-bonding interactions, the coulomb and van de Waals interactions were calculated by the Ewald and atom-based methods, respectively, with a cut-off of 18.5 Å. The methanol molecule geometry was optimized using the same methodology that the drug. Different conformations of the optimized ciprofloxacin drug and different relative orientations between the drug and the clay were randomly explored, both inside the halloysite nanotube and on the external surface of the clay. For this purpose, Monte Carlo methods using the Compass FF with Adsorption Locator module was used (BIOVIA, 2016). The more stable drug-clay complexes were selected when the ciprofloxacin is adsorbed on the inner surface and on the outer surface of the halloysite nanotube. Later, in both

selected adsorption models, a calculation was performed to fill the model with previously optimized methanol molecules using the Compass FF with Amorphous Cell module (BIOVIA, 2016). In this way, the methanol with a density of 0.792 g/cm³ filled the adsorption complexes (500 molecules of methanol), as it happened experimentally. These complexes were optimized fixing the structure of the clay, except the hydrogen atoms of the inner surface of halloysite with a cut-off of 18.5 Å. The adsorption energies of these complexes were compared according to the equation $\Delta E_{\text{ads}} = (E_{\text{drug}} - E_{\text{drug/clay}}) - (E_{\text{drug}} + E_{\text{clay}})$. For this, the energy of each optimized adsorption complex was calculated, as well as the drug and the clay with the solvent of the optimized complexes were isolated and the energies were calculated, with an energy calculation with the Compass FF, the Forcite program and a cut-off of 18.5 Å (BIOVIA, 2016).

2.7. Kinetic Release

The release of Cipro from Hal both in Hal/Cipro and Hal-Cipro was done as follows: 20 mg of the sample were dispersed in 1 mL of dissolution medium (phosphate buffers pH 7.4 and 5.5) and transferred into a sealed dialysis membrane (Medicell International Ltd MWCO 12-14000 with a diameter of 21.5 mm). Subsequently the membrane was put in a round bottom flask containing 9 mL of the release medium at 37°C and stirred. At fixed time, 1 mL of the release medium has been withdrawn and analyzed by UV-*vis* measurements. To ensure sink conditions, 1 mL of fresh solution has been used to replace the collected one.

2.8. Cipro release from gel matrix.

Hybrid hydrogels obtained at 3 wt % of Ht and 5 wt% of modified Hal were prepared, as discussed above, in a total volume of 3 mL. 3 mL of the phosphate buffer pH 5.5 or pH 7.4 were casted on gel matrix. The release kinetic was carried out at 37°C. At fixed intervals of time, 750 µL of supernatant solution were taken out to be spectrophotometrically analyzed controlling Cipro peak

at 320 nm, and simultaneously refilled with other 750 μ L of the same release medium pre-warmed at 37°C.

Total amounts of drug released (F_t) were calculated as follows:

$$F_t = V_m C_t + \sum_{i=0}^{t-1} V_a C_i \quad (\text{Eq. 4})$$

where V_m and C_t are the volume and the concentration of the drug at time t . V_a is the volume of the sample withdrawn and C_i is the drug concentration at time i ($i < t$).

2.9. Cytotoxicity Test (MTT assay)

NHDF were seeded in 96-well plates (0.35×10^5 cell/well in 200 μ L/well) and incubated for 24 h at 37°C in a humidified atmosphere containing 5% CO_2 (CO_2 Incubator, PBI International, Milan, I). After 24h, the medium was removed, cells were washed once with 200 μ L/well PBS (phosphate saline buffer, Sigma-Aldrich, I), and then treated for 24 h. Four different concentrations of ciprofloxacin for each nanomaterial were evaluated (5, 10, 25 and 100 μ M). These were compared with the free drug diluted at the same concentrations in growth medium (drug stock solution in 0.1 N HCl to allow drug solubilization). Eight replicates for each sample were performed. After 24 h of treatment, samples were withdrawn, fibroblasts washed once with PBS and exposed for 3 h to 50 μ l MTT solution (2.5 mg/mL solubilized in DMEM w/o red phenol) diluted in 100 μ L of DMEM. Then, the reagent was removed, cells washed and 100 μ L DMSO were pipetted in each well. The absorbance at 570 nm, with 690 nm as reference wavelength, was immediately read by means of an ELISA plate reader (FLUOstar Omega - BMG LabTech, G). Cell viability was calculated as percentage ratio between the absorbance of each sample and the absorbance of control, cell substrates in growth medium, GM.

2.10. Cell morphology

Cell morphology was evaluated using CLSM analysis. Briefly, cover slides with $\varnothing=13$ mm were placed on the bottom of the wells of a 24-well plate and 10×10^5 cells/well (400 μL /well) were seeded. After 24 h, cells were incubated for further 24 h with Cipro loaded nanomaterials and free Cipro (concentration 10 μM). Cells were fixed with 3% (w/v) glutaraldehyde for 2 h at room temperature. Cellular substrates were washed twice in PBS and cytoskeleton was stained with 150 μL (50 $\mu\text{g}/\text{mL}$) phalloindin-Atto 488 (Sigma-Aldrich, I) incubated for 40 min at room temperature, in the dark. After two-time washing with PBS, cell nuclei were stained with 100 μL of Iodide Propidium, (25 $\mu\text{g}/\text{mL}$) for 2 min in the dark, then samples were placed on a microscope slide and imaged using a Confocal Laser Scanning Microscope (CLSM, Leica TCS SP2, Leica Microsystems, I) using $\lambda_{\text{ex}} = 535\text{nm}$ and $\lambda_{\text{em}} = 617$ nm for Iodide Propidium and $\lambda_{\text{ex}} = 501$ nm and $\lambda_{\text{em}} = 523$ nm for phalloindin-Atto 488. The acquired images were processed with the software associated with the microscope (Leica Microsystem, LASX, CMS, GmbH, I).

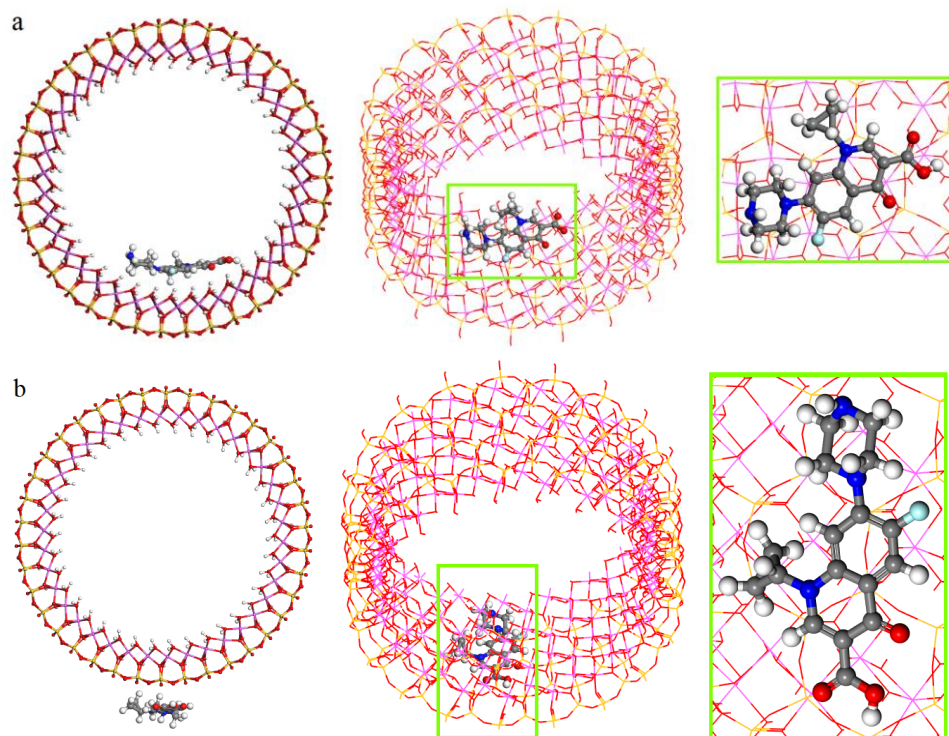
3. RESULTS AND DISCUSSION.

3.1. Loading of Cipro on Hal: supramolecular binding (Hal/Cipro)

Ciprofloxacin is an insoluble drug in water. To build optimal ciprofloxacin carrier systems based on HT/Hal hybrid hydrogels with high entrapment efficiency and high stability of the drug in water, we first performed preliminary investigation on the drug adsorption ability of Hal by of quantum mechanics calculations along with classical mechanics calculations and by the construction of the adsorption isotherms.

To investigate the nature of the ciprofloxacin adsorption on Hal we performed some molecular modelling simulations,(Prishchenko et al., 2018) considering both the internal and external Hal surface and methanol (MeOH) as solvent.

250 Monte Carlo methods using the Compass Force Field (FF) were performed to explore the more
251 stable halloysite/Cipro interaction on the two surfaces of the halloysite nanotube model (on the
252 inner and on the outer surfaces). The most stable model, with ciprofloxacin absorbed on the inner
253 clay surface, was selected (Figure 1a). In the same way, the most stable model when the drug is
254 adsorbed on the external surface was also selected (Figure 1b).



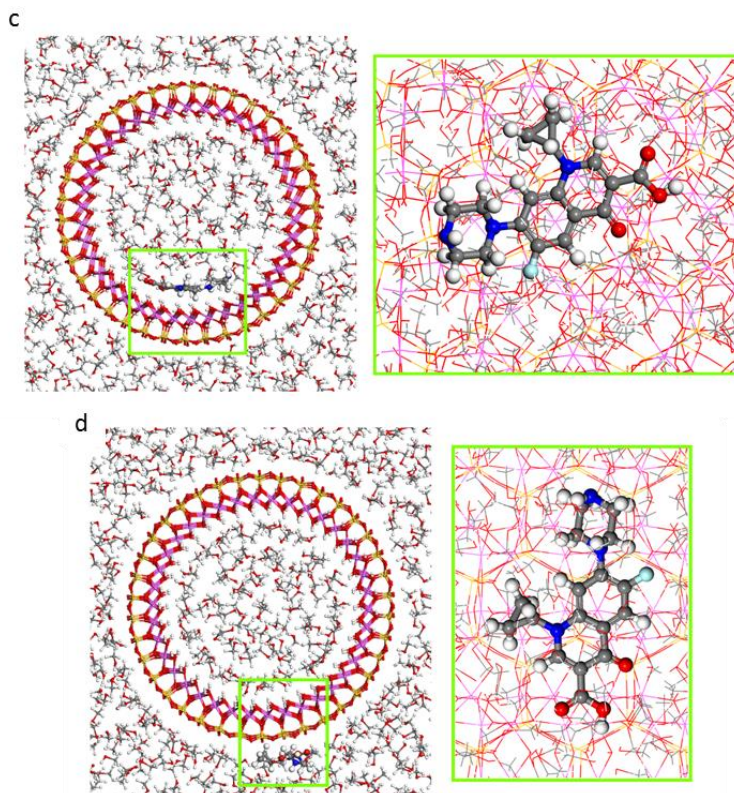


Figure 1. Adsorption models of the ciprofloxacin drug adsorbed on the internal (a-c) and external (b-d) surfaces of halloysite nanotube without or with methanol as solvent optimized with Monte Carlo method and Compass FF, views from (001) and (100) planes. The atoms of silicon, aluminium, hydrogen, carbon, nitrogen, oxygen, and fluorine are presented in yellow, pink, white, grey, blue, red, and cyan, respectively.

In the most stable adsorption model (Figure 1), the ciprofloxacin inside the halloysite was oriented in a perpendicular direction with respect to the c axis of the nanotube (Figure 1a). On the contrary, the drug on the external surface of the clay adopted a parallel position with respect to the c axis (Figure 1b).

Subsequently, the optimization of the adsorption models was performed filling previously each model with 500 optimized molecules of methanol by the Compass FF (Figure 1c-d). In these calculations, the structure of the halloysite previously optimized with Density Functional Theory (DFT) was fixed (Borrego-Sánchez et al., 2018), except the hydrogen atoms of the inner surface of the halloysite. In both cases, the ciprofloxacin maintained the same conformation that the adsorption complexes without solvent as it can be seen in Figure 1c-d.

273 In the adsorption model where the ciprofloxacin was adsorbed on the inner surface of the clay
 274 (Figure 1c), the mainly interaction between the drug and halloysite were hydrogen bonds, between
 275 the oxygen of the carbonyl groups and the hydrogens of the internal surface of the halloysite with
 276 $d(\text{COc}\dots\text{HOAl}) = 1.93\text{-}2.00 \text{ \AA}$, and between the nitrogen of the ciprofloxacin and the hydrogen of
 277 the internal surface of the halloysite with $d(\text{Nc}\dots\text{HOAl}) = 2.43 \text{ \AA}$. Also, hydrogens bonds between
 278 the drug and methanol solvent were found, specifically between the carbonyl O atoms of the drug
 279 and the hydroxyl H atom of methanol with $d(\text{COc}\dots\text{HOMe}) = 1.78\text{-}1.80 \text{ \AA}$, and between the
 280 hydrogens of the ciprofloxacin molecule and the oxygen of the hydroxyl group of methanol with
 281 $d(\text{Hc}\dots\text{OHMe}) = 1.86\text{-}1.96 \text{ \AA}$. Moreover, electrostatic interactions were showed between the C
 282 atoms of the ciprofloxacin and the hydrogens of the internal surface of the halloysite with
 283 $d(\text{Cc}\dots\text{HOAl}) = 2.35\text{-}2.51 \text{ \AA}$, and between the hydrogens of the drug and the oxygens of the
 284 halloysite with $d(\text{Hc}\dots\text{OHAl}) = 2.24\text{-}2.34 \text{ \AA}$.
 285 In the adsorption model where the ciprofloxacin was adsorbed on the outer surface of the halloysite
 286 nanotube (Figure 1d), hydrogen bonds were found only between the drug and the methanol
 287 molecules, in particular between the nitrogen of the amine group of the drug and the hydrogens of
 288 methanol with $d(\text{HNc}\dots\text{HOMe}) = 1.85 \text{ \AA}$, and between the hydrogens of the ciprofloxacin and the
 289 oxygen of methanol with $d(\text{Hc}\dots\text{OHMe}) = 1.80\text{-}2.07 \text{ \AA}$. Additionally, hydrogen bonds were
 290 showed between the fluorine atom and the hydrogen atom of methanol $d(\text{Fc}\dots\text{HOMe}) = 2.22 \text{ \AA}$,
 291 and between the oxygen of the carbonyl group of the drug and the hydrogen of methanol with
 292 $d(\text{COc}\dots\text{HOMe}) = 1.86 \text{ \AA}$. Furthermore, electrostatic interactions were observed such as between
 293 the hydrogens of the drug and the oxygens of the external surface of halloysite with $d(\text{Hc}\dots\text{OSi})$
 294 $= 2.47\text{-}2.49 \text{ \AA}$.

Lastly, the adsorption energies of both models were compared according to the equation $\Delta E_{\text{ads}} = (E_{\text{drug/clay complex}}) - (E_{\text{drug}} + E_{\text{clay}})$. The results showed that both adsorption models presented a negative adsorption energy. Therefore, the adsorption of the drug is favorable both on the internal and external surface of the halloysite nanotube. Comparing both adsorption complexes, the most stable is one in which the ciprofloxacin molecule is adsorbed on the inner surface of the halloysite. Specifically, the energy of adsorption of the complex with the drug on the internal surface of the clay is 14.5 kcal/mol more stable than when ciprofloxacin is adsorbed on the external surface of the nanotube.

Adsorption studies in different media (see SI) confirmed that halloysite nanotubes showed the highest adsorption capacity towards Cipro in MeOH, in agreement with the computational results. In these conditions, where the drug is insoluble, the main effect should be a hydrophobic effect, which maximize the interaction with the Hal lumen, increasing the adsorption efficiency.

Based on the above results, loading of ciprofloxacin into pristine Hal was carried out by vacuum cycling of a Hal methanolic suspension in a ciprofloxacin acidic solution (HCl 0.1 N). This cycle was repeated several times to obtain the highest loading efficiency (Figure 2). After loading, the Hal/Cipro filler was washed several times with methanol to remove free drug molecules. The loading of ciprofloxacin molecules loaded into the Hal carrier, estimated by TGA, was ca. 2.6 wt%.

According to the densities of the pure components (2.53 and 1.5 g cm⁻³ for Hal and ciprofloxacin, respectively) 2.6 wt% of Cipro corresponds to a volume loading of 4.4% in the Hal/Cipro filler.

3.2. Loading of Cipro on Hal: covalent grafting (Hal-Cipro).

To obtain a pH-sensitive carrier system for wound healing and to improve the drug loading onto Hal, the ciprofloxacin molecules were also covalently grafted on Hal external surface (Figure 2).

In details, the synthesis of ciprofloxacin modified clays was carried out by N,N-dicyclohexylcarbodiimide-catalyzed amide condensation of Cipro units to Hal-NH₂ (0.5 mmol/g loading of -NH₂ groups) by forming an amide bond that afforded hybrid materials with a loading of ca. 16 ± 0.1 wt% (0.48 mmol/g of ciprofloxacin molecules) estimated by TGA, with respect to starting material.

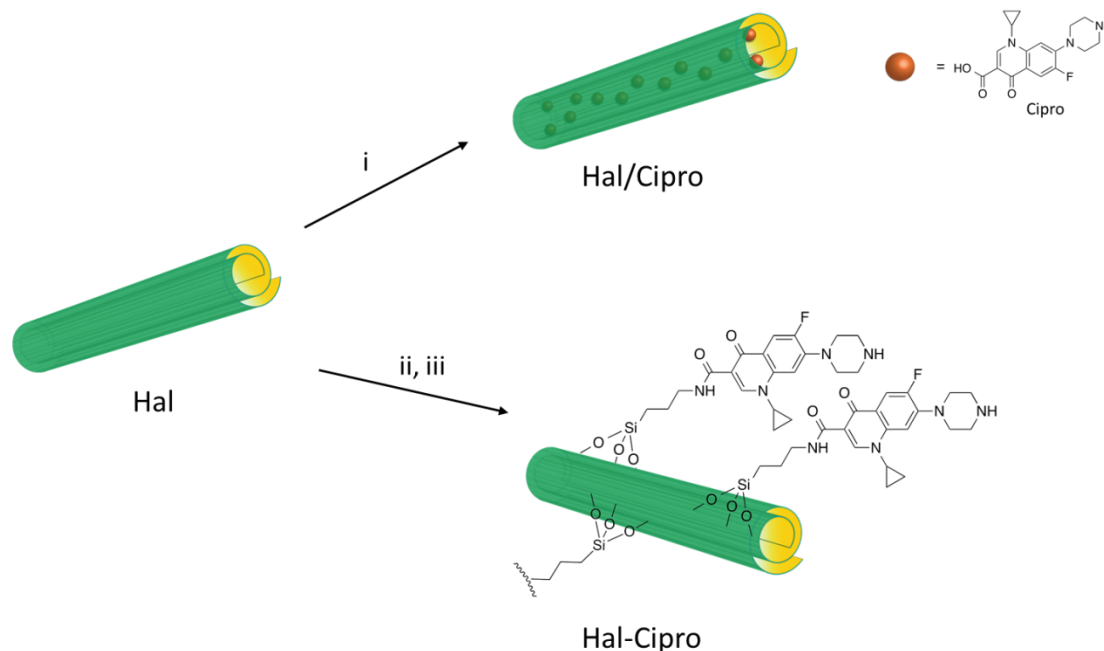


Figure 2. Schematic representation of the synthesis of Hal/Cipro and Hal-Cipro nanomaterials. Synthetic route: (i) ciprofloxacin, MeOH, vacuum, 18 h, r.t., (ii) APTES, toluene, reflux, 48 h, (iii) ciprofloxacin, DCC, CH₂Cl₂, r.t., 3 d.

3.3. Physico-chemical characterization of Hal/Cipro and Hal-Cipro fillers.

Hal/Cipro and Hal-Cipro fillers were characterized by FT-IR spectroscopy and thermogravimetric analysis (TGA). The spectroscopic study showed that both nanomaterials present, in their FT-IR spectra (see SI) the typical Hal vibration stretching bands (Massaro et al., 2018a). The FT-IR spectrum of Hal/Cipro shows, beside the Hal bands, some stretching bands of ciprofloxacin (Figure S.1b). In particular, the band at ca. 1539 cm⁻¹ related to the C=O stretching of quinolone moiety

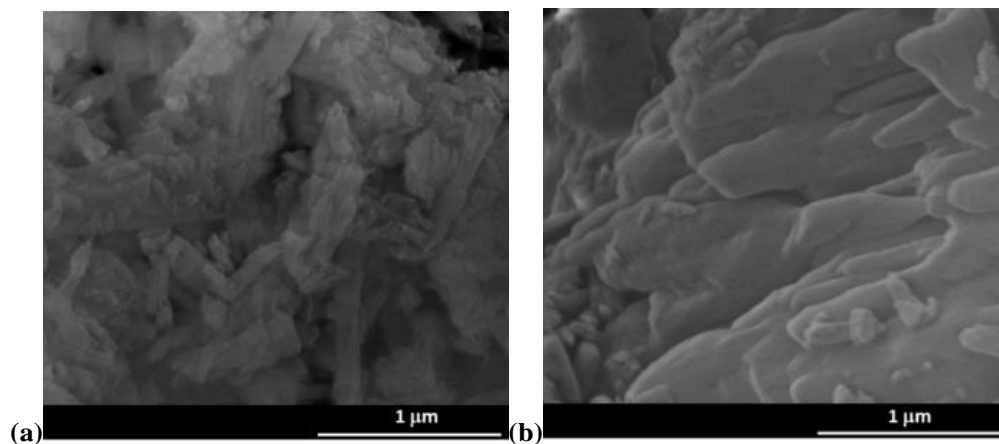
and the bands around 1483 and 1435 cm^{-1} due to the stretching of the C–N groups. On the contrary, the FT-IR spectrum of the ciprofloxacin covalently linked to the Hal external surface is quite different. Indeed, in this case, beside the typical vibration bands, new peaks are present which confirm the successful linkage.

Specifically, it is possible to observe the band at ca. 3320 cm^{-1} related to stretching of the N–H group of the amide bond and the band at ca. 1612 cm^{-1} which superimposed the typical band of Hal, due to the stretching of the amide C=O.

In addition, the stronger intensities of the ciprofloxacin bands in the Hal-Cipro compared to those in Hal/Cipro confirm the high loading obtained after the covalent grafting.

As stated above the ciprofloxacin amount loaded onto Hal fillers was estimated by TGA. TGA data highlighted that the Cipro content is much larger in Hal-Cipro that also shows a larger hydration with respect to Hal/Cipro. The mass loss due to Cipro degradation starts at ca. 250°C in both cases.

The morphology of the two different nanomaterials was imaged by SEM and TEM investigations (Figure 3). After the ciprofloxacin loading, the characteristic lengths, and the tubular shape of Hal are preserved in the sample (Figures 3a and S.3); on the contrary, the grafting of Cipro molecules on the external Hal surface causes a change in the morphology (Figure 3b).



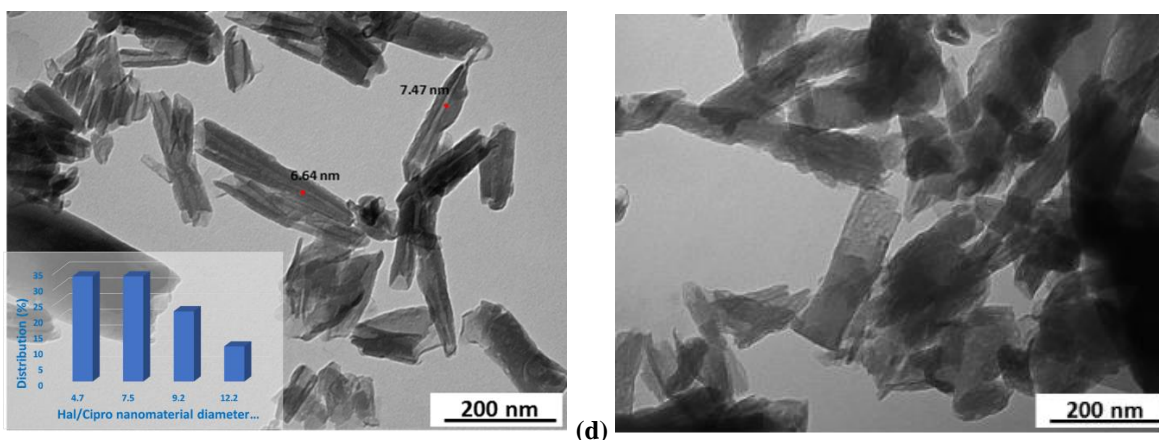


Figure 3. (a-b) SEM and (c-d) TEM images of (a, c) Hal/Cipro (the inset shows the Hal/Cipro diameter size distribution (n = 20)) and (b, d) Hal-Cipro fillers.

In this case, we found rather compact structures, where the tubes are not observable, probably due to the large amount of ciprofloxacin grafted onto the HNTs external surface, which interact each other by π - π and hydrogen bonding interactions.

Furthermore, TEM images confirm the different morphology of Hal/Cipro and Hal-Cipro fillers. In the TEM image of Hal/Cipro filler (Figure 3c) the lumen is not apparent in all its length (see red mark in Figure 3c) and exhibits a decreased diameter in comparison to pristine Hal (Massaro et al., 2018a); i.e., from 14.9 nm to ca. 7.3 ± 2.6 nm. On the contrary, in Hal-Cipro filler (Figure 3d) the external Hal surface seems to be rougher and less defined with respect to those of pristine nanotubes (Figure S.3), indicating the presence of organic matters.

3.4. Study of gel properties

As known hectorite can form stable hydrogels in aqueous media due to the formation of delaminated dispersions by the self-assembling of its nanodisk via face-edge aggregation. Furthermore, it is reported that the introduction of pristine halloysite filler, in Ht hydrogel, helps the gel formation with an improvement of the rheological properties (Massaro et al., 2019a). Therefore, herein we studied the effect of the covalent modified Hal on the rheological properties

of Ht hydrogels. To perform these studies a series of different hydrogels were prepared by varying the concentration of gelator (from 2 wt% to 10 wt%) and filler (from 2 wt% to 7 wt%). The experimental data showed that the Ht/Hal hydrogels more stable were form at concentration of 5 wt% of both gelator and filler.

Figure 4 shows the effect of increasing strain amplitude on the storage and loss modulus of the hectorite hydrogels (Ht and Ht/Hal-Cipro, respectively). The behavior of the studied gels was very similar. Both pristine hectorite hydrogels and the hybrid one (Ht/Hal-Cipro) showed strain-induced gel–sol transitions with initial critical high-modulus gel at low strains transforming to a low modulus liquid at high strains. Pristine hectorite hydrogels were quite strong at 5 wt % with G' ($\gamma \rightarrow 0$) ~ 550 Pa, increasing to ~ 600 Pa by the presence of Hal. Storage and loss moduli crossed at $\sim 8\%$ strain in both pristine and hybrid hydrogels. Our results are similar to those observed by Annemieke et al. (ten Brinke et al., 2007, 2008), with hectorite hydrogels in presence of small amounts of rod-like particles of boehmite.

Accordingly, the increase in the linear region of the G' curves of our hydrogels can be explained by the addition of a more strain-sensitive component (rod-shape particles of Hal) resulting in the observed enhancement of the hydrogel structure.

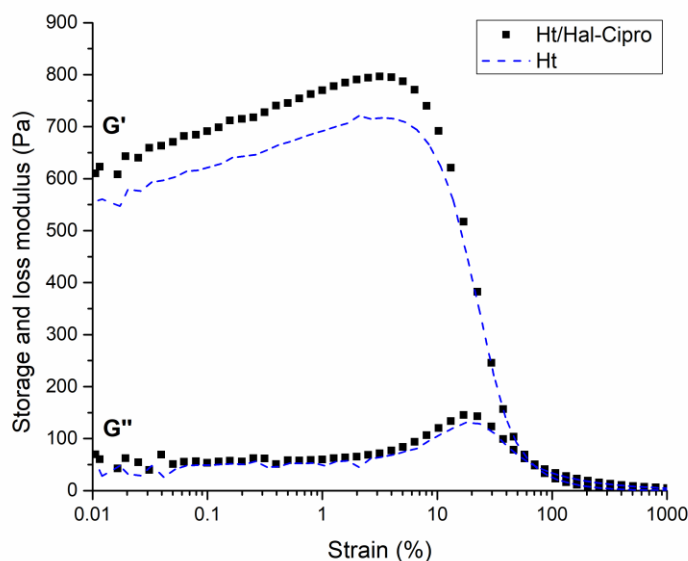


Figure 4. Amplitude sweeps for the Ht/Hal-Cipro hybrid hydrogel compared to pristine hectorite one at the same solid concentration.

3.5. Kinetic Release

The kinetic release of Cipro molecules from both Hal fillers and from the hybrid hydrogels was performed both at skin's pH (5.4) and under neutral conditions (pH 7.4).

3.5.1. Ciprofloxacin release from Hal fillers.

As far as is regarding the ciprofloxacin release from the Hal fillers we found that at pH 5.4 (Figure 5) a sustained release of Cipro from the supramolecular Hal/Cipro filler (Figure 5a) was achieved, with ca. 20 wt% of the total amount of drug molecules loaded released in 24 h. Different behaviour was obtained in the case of Hal-Cipro, where the drug is grafted onto Hal surface by a pH sensitive bond. In this case, after the hydrolysis of amide bonds, the ciprofloxacin is quantitatively released within 75 min (Figure 5b).

At pH 7.4 (Figure 5), both systems exhibited sustained release of Cipro with an initial rapid-release phase, followed by a gradually slower release pattern. In particular, the Cipro showed a slower

release from Hal/Cipro nanomaterial, where only 30% of the total amount of drug molecules loaded into Hal lumen is released after 24 h (Figure 5a); on the contrary, ca. 60% of Cipro of the total amount of Cipro grafted onto halloysite is released in the case of Hal-Cipro (Figure 5b). It is noteworthy that in the same conditions the free drug spread through the dialysis membrane almost totally within few minutes (data not shown) indicating that release of Cipro from solution through the dialysis membrane is a fast process according to that already reported for other biologically active molecules (Massaro et al., 2021a).

The kinetic data obtained were analyzed by a first order, double exponential (DEM) and Korsmeyer–Peppas models to deep investigate the release behavior of Cipro from the two different fillers. The results showed that at pH 5.4 the release of ciprofloxacin from Hal-Cipro filler follows the first order model ($M_{\infty} = 109 \pm 8 \text{ wt\%}$; $k = 0.029 \pm 0.008 \text{ min}^{-1}$, $R^2 = 0.9712$) indicating that after the cleavage of the amide bond, the diffusion of the molecule occurs through the dialysis membrane. Conversely, the release of ciprofloxacin from Hal/Cipro is ruled by a Fickian mechanism, therefore following a Power fit model ($k = 4.4 \pm 2.9 \text{ min}^{-1}$; $n = 0.24 \pm 0.07$, $R^2 = 0.9683$). At pH 7.4, the release of Cipro from Hal/Cipro nanomaterial follows a first order model, in agreement with a slow diffusion from Hal lumen ($k = 0.0037 \pm 0.0003 \text{ min}^{-1}$), whereas the Cipro release from Hal-Cipro is better fitted by a DEM model. According to the literature, the DEM describes a mechanism consisting of two parallel reactions involving two distinguishable species. Based on these findings, we hypothesized that might exist favorable π – π interactions between the Cipro molecules grafted onto the external Hal and some free drug molecules which did not take part in the amide condensation. Due to the strong supramolecular interactions, these free molecules were not removed during the work-up of the reaction (Figure 5c). Therefore, it is possible to suppose a faster release of Cipro because of the diffusion of Cipro molecules supramolecular

interacting ($k_I = 0.10 \pm 0.01 \text{ min}^{-1}$) and a slow release of the covalently linked ones, due to the slow hydrolysis of amide bond in neutral conditions ($k_I = 0.0046 \pm 0.0006 \text{ min}^{-1}$). By the fitting of the kinetic data, we calculated the amount of ciprofloxacin supramolecular interacting onto Hal corresponding to ca. 4 wt% in comparison to the total ciprofloxacin loading (16 wt%) in the Hal-Cipro.

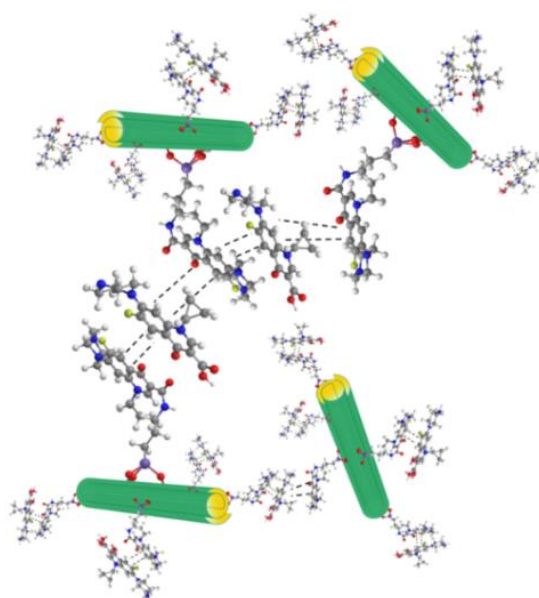
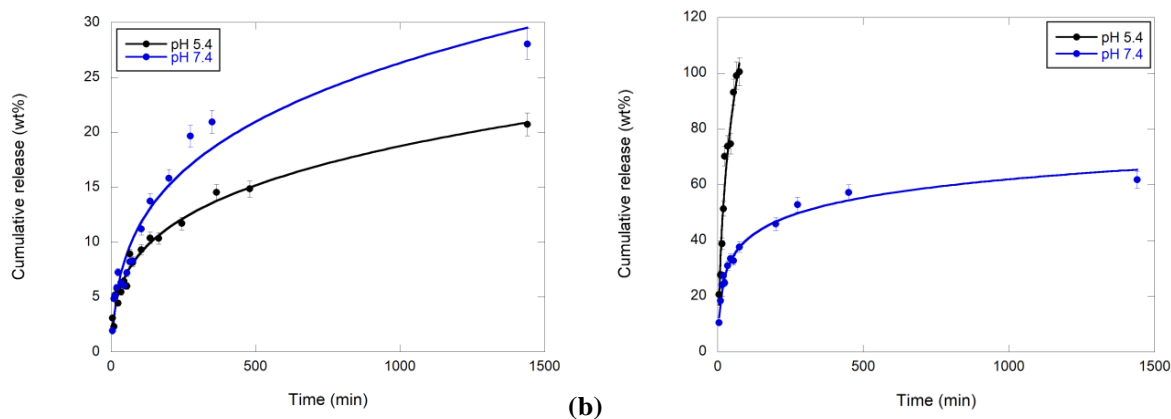


Figure 5. Kinetic release of ciprofloxacin from (a) Hal/Cipro and (b) Hal-Cipro nanomaterials in phosphate buffer (0.05 M) solution at pH 5.4 and pH 7.4, at 37°C; (c) cartoon representation of the interaction existing between “free” ciprofloxacin and Hal-Cipro filler.

437 To prove this hypothesis, we performed some XRD and DSC measurements (Figure 6). In Figure
438 6a are reported the XRD spectra of ciprofloxacin, Hal/Cipro, and Hal-Cipro.

439 All nanomaterials showed the typical reflections of Hal (Aguzzi et al., 2019), namely the
440 reflections at 2θ 12°, 20°, 25°, 35, 54 and 62 corresponding to the planes (001), (100), (002), (100),
441 (210) and (300) respectively, matching with the JCPD card no. 00-029-1487. After the covalent
442 linkage of the Cipro on the clay, all reflection peaks remain unchanged indicating that no clay
443 structural variation occurs, confirming that the covalent linkage occurs only on the Hal external
444 surface without intercalation. In addition, typical XRD features of ciprofloxacin are clearly
445 observable in the fillers. Thus, XRD profile of Hal-Cipro confirmed the presence of some Cipro
446 molecules recrystallized on the Hal surfaces (sharp peaks in the range of 10°–40° confirms the
447 presence of the crystalline form of Cipro). On the contrary, the XRD profile of Hal/Cipro is almost
448 consistent with the XRD feature of pristine Hal. This evidence indicates that the interaction
449 between Hal and ciprofloxacin and that the whole process of preparation does not disturb the
450 structure of Hal and once again no exfoliation of the clay occurs.

451 In Figure 6b the DSC thermograms of Cipro (free drug), Hal/Cipro and Hal-Cipro fillers are
452 showed. The DSC profile of Cipro exhibited a sharp endothermic peak due to the melting of the
453 drug molecules, in the boundary 264-270°C (centered at 268.6°C). As it reported, pristine Hal
454 shows a wide endothermic phenomenon, in the range 50–120°C, ascribed to the dehydration of
455 physisorbed water and interlayer water, followed by another endothermic band (270–320°C)
456 (Aguzzi et al., 2019). The Hal/Cipro filler showed the typical peaks in the thermograms related to
457 the endothermic processes of Hal. In addition, some minor Cipro degradation events were observed
458 at ca. 160°C, 225°C and 255°C. These results demonstrated that Cipro molecules are not in its
459 crystalline form after loading into Hal lumen (Silva et al., 2020). On the contrary, the DSC

thermogram of Hal-Cipro filler evidenced the presence of two significant endothermic peaks centered at ca. 232 and 267°C. This finding further confirms the remaining unreacted Cipro recrystallized on Hal external surface.

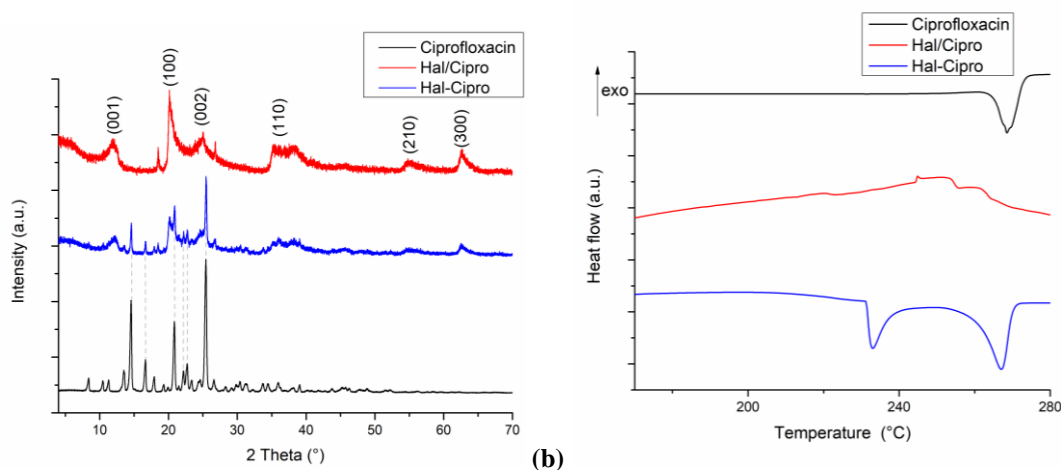


Figure 6. (a) XRD patterns of ciprofloxacin, Hal/Cipro and Hal-Cipro fillers and (b) DSC profiles of ciprofloxacin, Hal/Cipro and Hal-Cipro fillers.

3.5.2. Ciprofloxacin release from the hybrid hydrogels

The release of Cipro from the hybrid hydrogels was also studied to verify if incorporation of Hal into the gel matrix could induce a time-controlled drug release process at skin's pH (5.4) and under neutral conditions (pH 7.4). To make a proper comparison, we also prepared a Ht hydrogel in the presence of ciprofloxacin alone (5 wt% of ciprofloxacin with respect to Ht). In this case, no gel formation occurred even after 48 h (Figure S.5). It could be probable that ciprofloxacin interacts by cation exchange with the Ht interlayers, as already found with similar inorganic excipients, disturbing the gelation process (Wang et al., 2011; Wu et al., 2013). This result confirms the crucial role played by the halloysite fillers in the Ht matrix as carrier for the sustained release of drugs.

The trends of cumulative Cipro release from the hybrid hydrogels as a function of time are displayed in Figure 7. In the case of Hal/Cipro filler, at both pH values, a similar release pattern

was observed. We found a slow release of the drug from the hybrid hydrogels for the first 200 min (Figure 7a), afterwards, we observed the dissolution of the gel matrix. In this case, since there is not the influence of the gel matrix, it was assumed that the Cipro kinetic release should be very similar to that from pristine halloysite filler (see above). Conversely, the introduction of Hal-Cipro filler in the Ht hydrogel led a slower release pattern of the Cipro without no relevant differences between the two media investigated. Also in this case the ciprofloxacin covalently grafted onto the external surface of halloysite could interact once again by cation exchange with the Ht interlayers and this, could hamper the drug release as already reported for similar clays (Chen et al., 2015). The small amount of ciprofloxacin released from the gel corresponded to the drug molecules recrystallized on Hal external surface, which spread through the hydrogel (Figure 7b). Cipro molecules released from the Hal and then sorbed into the Ht interlayer will not easily exchanged by cations. Interestingly, permanence of Cipro in the gel is consider a positive matter, as it has been demonstrated that Cipro loaded in similar nanoclays vehicles (montmorillonite) significantly inhibited bacteria growth compared to free drug molecules (Chen et al., 2015). Furthermore, since frequent medical treatment or manipulation over a wounded area could impair/interrupt new tissue formation, a sustained release of antibiotic could potentially reduce the number of applications needed over time and, allow lesions to heal faster.

In this case, the experimental data are better fitted by a Higuchi model ($k = 0.43 \pm 0.01 \text{ min}^{-1}$, $R^2 = 0.9897$) for kinetic data obtained at pH 7.4, whereas the Cipro release from the Ht/Hal hybrid hydrogel follows the Power fit model at pH 5.4 ($k = 1.7 \pm 0.4 \text{ min}^{-1}$, $n = 0.19 \pm 0.02$, $R^2 = 0.9945$).

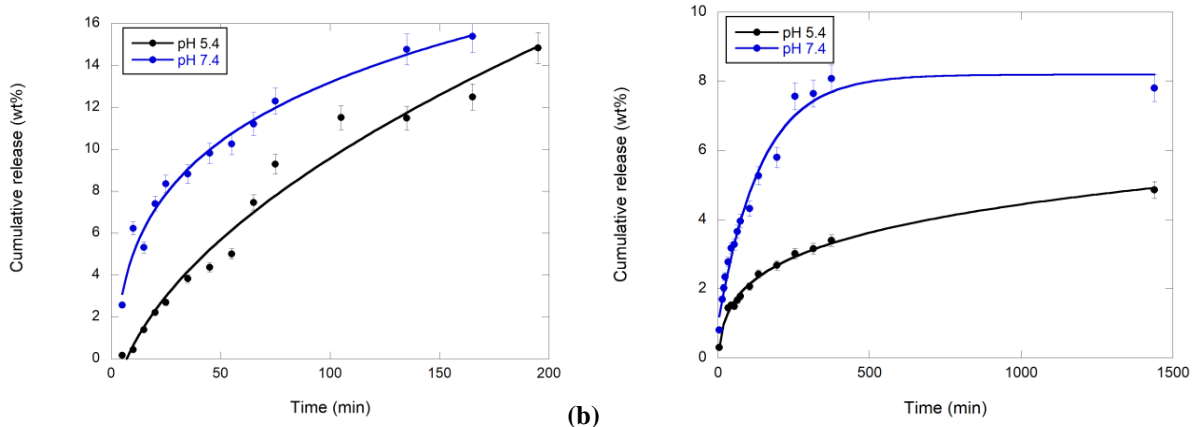


Figure 7. Kinetic release of ciprofloxacin from (a) Ht/Hal/Cipro hybrid hydrogel and (b) Ht/Hal-Cipro hybrid hydrogel phosphate buffer (0.05 M) solution at pH 5.4 and pH 7.4, at 37°C.

3.6. Cytocompatibility

It is reported that Ht hydrogels did not possess cytotoxic effects on normal human dermal fibroblasts within 24 h (García-Villén et al., 2021). Thus, we studied the effects on the same cell lines of the Hal fillers obtained in this study.

Figure 8 reports the % viability of fibroblasts after 24 h contact with Hal-Cipro and Hal/Cipro fillers at different concentrations compared to ciprofloxacin (free drug) as reference and the control, GM, corresponding to standards growth conditions. Pristine Hal did not show any cytotoxicity in the concentration range investigated (Sandri et al., 2020).

A dose-dependent and statistically significant decrease in cell viability was particularly evident for cells treated with Cipro as free drug. Besides the increasing amount of the free quinolone used (Shi et al., 2018), the viability reduction could be related to the cell sensitivity to the acidic pH of Cipro sample (drug stock solution in 0.1 N HCl to allow drug solubilization).

Hal/Cipro causes a statistical viability reduction at concentrations higher than 25 μ M. Despite this, as shown from the results, the sample containing Cipro at 100 μ M lead to 60% cell viability higher than that of the free drug at the same concentration (40%), suggesting no additional cytotoxic

effects. When cells were exposed to covalent halloysite-ciprofloxacin composites (Hal-Cipro), no statistically dose-dependent cytotoxicity occurred with a 90% viability up to 25 μ M.

This could be related to the different release kinetic from Hal at pH 7.4 (pH of growth medium). Hal-Cipro is characterized by a cytocompatibility strongly influenced by drug concentration in the nanomaterial since about 60% of the drug is released in the medium, while Hal/Cipro shows a less marked influence of concentration on cytocompatibility, and this could be due to a lower drug release (about 20% in 24 h).

In Figure 9, Confocal Laser Scanning Microscopy (CLSM) photographs of fibroblasts treated with 10 μ M of free ciprofloxacin and ciprofloxacin loaded carriers are reported.

The fusiform shape of fibroblasts was totally preserved and no differences among each sample occurred, confirming the sample biocompatibility at concentration used. Although it was not possible to localize the drug moiety and to study the Hal and drug cell uptake, the results confirm a positive cell-sample interaction. F-actin filaments of the cytoskeleton are well organized (Phalloidin FITC staining in green), and the nuclei (Iodine Propidium staining in red) are normal.

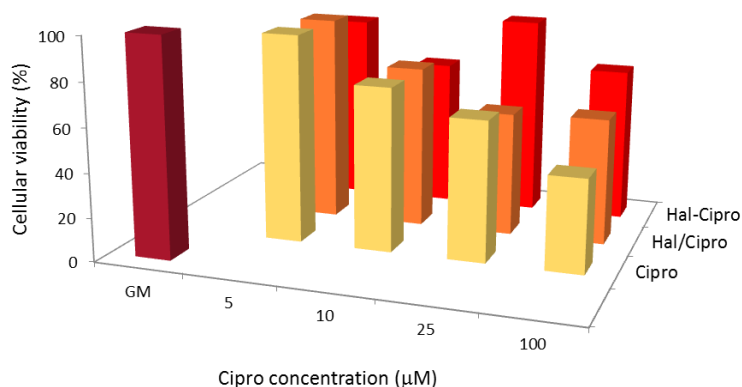


Figure 8. % viability of fibroblasts after 24 h contact with Hal-Cipro and Hal/Cipro samples at different concentrations of ciprofloxacin in the nanomaterials compared to ciprofloxacin (free drug) as reference and the control, GM, corresponding to standards growth conditions (means values \pm es; n=8) (see ESI for error bars).

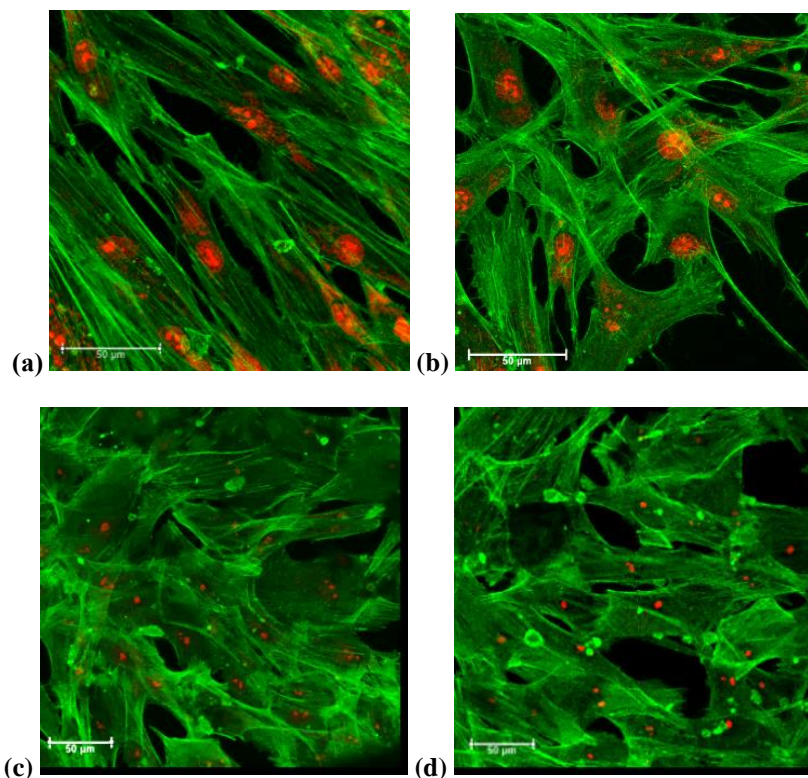


Figure 9. CLSM images of fibroblasts after 24 h culture in (a) GM (standard growth conditions); (b) Cipro; (c) Hal/Cipro and (d) Hal-Cipro, Cipro concentration 10 μ M.

CONCLUSIONS

In summary, in this paper, we pointed our attention to the development of ad hoc covalently modified halloysite as filler for Ht hydrogels. The introduction of such fillers into the gel matrix indeed, was crucial to achieve a sustained release of ciprofloxacin for potential wound healing applications.

To achieve this objective, firstly, we studied the ciprofloxacin loading onto Hal both by a supramolecular and covalent approach (Hal/Cipro and Hal-Cipro, respectively). The interaction between ciprofloxacin and halloysite was thoroughly investigated by several techniques and at molecular level by means of quantum mechanics calculations along with empirical interatomic potentials. Both fillers were characterized by FT-IR spectroscopy and TGA measurements which confirmed the successful loading and grafting of ciprofloxacin. The different morphologies of the

two fillers were imaged by SEM and TEM investigations. Rheological measurements highlighted that the introduction of modified Hal into the gel matrix improved its properties helping the gel formation.

Kinetic release experiments of the drug from Hal fillers at at skin's pH (5.4) and under neutral conditions (pH 7.4), showed that the release is strictly dependent to the pH.. Conversely the ciprofloxacin molecules were slowly released from the gel matrix at both pH, which could be important for further applications as transdermal systems.

Finally, both MTT test and CLSM investigations proved the absence of any relevant cytotoxic effects of the synthesized fillers on normal human fibroblast cell lines.

In conclusion, in view of the positive *in vitro* cytocompatibility and *wound healing* effects reported in the literature for both hectorite and halloysite future work will be devoted to further *in vitro* and *in vivo* studies to assess the feasibility of the novel systems to enhance wound healing and to effectively prevent bacterial for the treatment of chronic skin lesions.

Supporting Information. Ciprofloxacin adsorption studies onto Hal, FT-IR spectra and TGA analysis, TEM and SEM images of pristine Hal and Ht, UV-*vis* spectra of ciprofloxacin released, % viability of fibroblasts after 24 h contact with Cipro, Hal-Cipro and Hal/Cipro.

ACKNOWLEDGMENTS

The work was carried out in the frame of the PON “AIM: Attrazione e Mobilità Internazionale” No. 1808223-1 project. Authors are thankful to H.A. Duarte for providing atomic coordinates of halloysite, to the CSIC Computational Center and the University of Granada Computation Center for computation facilities, and the Andalusian project grants RNM-1897 and P18-RT-3786, and the Spanish MINECO projects, PCIN-2017-098, FIS2016-77692-C2-2-P and CGL2016-80833-R, for the financial support of this research.

Author Contributions

C.V.I and S.R. conceptualization, project administration, supervision, writing – review & editing, M.M. and A.B.-S. writing – original draft, M.M., A.B.S., R.S.E., G.C., F.G.-V., S.G., G.L., D.M., C.I.S.-D., G.S. formal analysis and investigation.

Funding

This research did not receive any specific grant from funding agencies in the public, commercial, or not-for-profit sectors.

REFERENCES

- Aguzzi, C., Donnadio, A., Quaglia, G., Latterini, L., Viseras, C., Ambroggi, V., 2019. Halloysite-Doped Zinc Oxide for Enhanced Sunscreening Performance. *ACS Appl. Nano Mater.* 2, 6575-6584.
- Alfieri, M.L., Massaro, M., d'Ischia, M., D'Errico, G., Gallucci, N., Gruttadauria, M., Licciardi, M., Liotta, L.F., Nicotra, G., Sfuncia, G., Riela, S., 2022. Site-specific halloysite functionalization by polydopamine: A new synthetic route for potential near infrared-activated delivery system. *J. Colloid Interface Sci.* 606, 1779-1791.
- Bellani, L., Giorgetti, L., Riela, S., Lazzara, G., Scialabba, A., Massaro, M., 2016. Ecotoxicity of halloysite nanotube-supported palladium nanoparticles in *Raphanus sativus* L. *Environ. Toxicol. Chem.* 35, 2503-2510.
- Borrego-Sánchez, A., Awad, M.E., Sainz-Díaz, C.I., 2018. Molecular Modeling of Adsorption of 5-Aminosalicylic Acid in the Halloysite Nanotube. *Minerals* 8, 61.
- Borrego-Sánchez, A., Hernández-Laguna, A., Sainz-Díaz, C.I., 2017. Molecular modeling and infrared and Raman spectroscopy of the crystal structure of the chiral antiparasitic drug Praziquantel. *J. Mol. Model.* 23, 106.
- Borrego-Sánchez, A., Viseras, C., Aguzzi, C., Sainz-Díaz, C.I., 2016. Molecular and crystal structure of praziquantel. Spectroscopic properties and crystal polymorphism. *Eur. J. Pharm. Sci.* 92, 266-275.
- Breda, S.A., Jimenez-Kairuz, A.F., Manzo, R.H., Olivera, M.E., 2009. Solubility behavior and biopharmaceutical classification of novel high-solubility ciprofloxacin and norfloxacin pharmaceutical derivatives. *Int. J. Pharm.* 371, 106-113.
- Bretti, C., Cataldo, S., Gianguzza, A., Lando, G., Lazzara, G., Pettignano, A., Sammartano, S., 2016. Thermodynamics of Proton Binding of Halloysite Nanotubes. *Journal of Physical Chemistry C* 120, 7849-7859.
- Campoli-Richards, D.M., Monk, J.P., Price, A., Benfield, P., Todd, P.A., Ward, A., 1988. Ciprofloxacin. *Drugs* 35, 373-447.
- Carazo, E., Borrego-Sánchez, A., García-Villén, F., Sánchez-Espejo, R., Aguzzi, C., Viseras, C., Sainz-Díaz, C.I., Cerezo, P., 2017. Assessment of halloysite nanotubes as vehicles of isoniazid. *Colloids Surf. B. Biointerfaces* 160, 337-344.

Chen, H., Gao, B., Yang, L.-Y., Ma, L.Q., 2015. Montmorillonite enhanced ciprofloxacin transport in saturated porous media with sorbed ciprofloxacin showing antibiotic activity. *J. Contam. Hydrol.* 173, 1-7.

Dawson, J.I., Oreffo, R.O.C., 2013. Clay: New Opportunities for Tissue Regeneration and Biomaterial Design. *Adv. Mater.* 25, 4069-4086.

Fakhrullina, G.I., Akhatova, F.S., Lvov, Y.M., Fakhrullin, R.F., 2015. Toxicity of halloysite clay nanotubes in vivo: a *Caenorhabditis elegans* study. *Environmental Science: Nano* 2, 54-59.

García-Villén, F., Sánchez-Espejo, R., Borrego-Sánchez, A., Cerezo, P., Sandri, G., Viseras, C., 2021. Assessment of Hectorite/Spring Water Hydrogels as Wound Healing Products. *Proceedings* 78, 6.

Gorbachevskii, M.V., Stavitskaya, A.V., Novikov, A.A., Fakhrullin, R.F., Rozhina, E.V., Naumenko, E.A., Vinokurov, V.A., 2021. Fluorescent gold nanoclusters stabilized on halloysite nanotubes: in vitro study on cytotoxicity. *Appl. Clay Sci.* 207, 106106.

Guimarães, L., Enyashin, A.N., Seifert, G., Duarte, H.A., 2010. Structural, Electronic, and Mechanical Properties of Single-Walled Halloysite Nanotube Models. *J. Phys. Chem. C* 114, 11358-11363.

Hu, H., Xu, F.-J., 2020. Rational design and latest advances of polysaccharide-based hydrogels for wound healing. *Biomater. Sci.* 8, 2084-2101.

Kevadiya, B.D., Rajkumar, S., Bajaj, H.C., Chettiar, S.S., Gosai, K., Brahmabhatt, H., Bhatt, A.S., Barvaliya, Y.K., Dave, G.S., Kothari, R.K., 2014. Biodegradable gelatin–ciprofloxacin–montmorillonite composite hydrogels for controlled drug release and wound dressing application. *Colloids Surf. B. Biointerfaces* 122, 175-183.

Korzeniowska, A., Strzempek, W., Makowski, W., Menaszek, E., Roth, W.J., Gil, B., 2020. Incorporation and release of a model drug, ciprofloxacin, from non-modified SBA-15 molecular sieves with different pore sizes. *Microporous Mesoporous Mater.* 294, 109903.

Kryuchkova, M., Danilushkina, A., Lvov, Y., Fakhrullin, R., 2016. Evaluation of toxicity of nanoclays and graphene oxide in vivo: a *Paramecium caudatum* study. *Environmental Science: Nano* 3, 442-452.

Liang, Y., Zhao, X., Hu, T., Han, Y., Guo, B., 2019. Mussel-inspired, antibacterial, conductive, antioxidant, injectable composite hydrogel wound dressing to promote the regeneration of infected skin. *J. Colloid Interface Sci.* 556, 514-528.

Lin, T., Zhao, S., Niu, S., Lyu, Z., Han, K., Hu, X., 2020. Halloysite nanotube functionalized with La-Ca bimetallic oxides as novel transesterification catalyst for biodiesel production with molecular simulation. *Energy Convers. Manage.* 220.

Liu, M., Jia, Z., Jia, D., Zhou, C., 2014. Recent advance in research on halloysite nanotubes-polymer nanocomposite. *Prog. Polym. Sci.* 39, 1498-1525.

Lvov, Y., Aerov, A., Fakhrullin, R., 2014. Clay nanotube encapsulation for functional biocomposites. *Adv. Colloid Interface Sci.* 207, 189-198.

Massaro, M., Barone, G., Barra, V., Cancemi, P., Di Leonardo, A., Grossi, G., Lo Celso, F., Schenone, S., Viseras Iborra, C., Riela, S., 2021a. Pyrazole[3,4-d]pyrimidine derivatives loaded into halloysite as potential CDK inhibitors. *Int. J. Pharm.*, 120281.

Massaro, M., Barone, G., Biddeci, G., Cavallaro, G., Di Blasi, F., Lazzara, G., Nicotra, G., Spinella, C., Spinelli, G., Riela, S., 2019a. Halloysite nanotubes-carbon dots hybrids multifunctional nanocarrier with positive cell target ability as a potential non-viral vector for oral gene therapy. *J. Colloid Interface Sci.* 552, 236-246.

656 Massaro, M., Buscemi, G., Arista, L., Biddeci, G., Cavallaro, G., D'Anna, F., Di Blasi, F., Ferrante,
 657 A., Lazzara, G., Rizzo, C., Spinelli, G., Ullrich, T., Riela, S., 2019b. Multifunctional Carrier Based
 658 on Halloysite/Laponite Hybrid Hydrogel for Kartogenin Delivery. *ACS Med. Chem. Lett.* 10, 419-
 659 424.
 660 Massaro, M., Casiello, M., D'Accolti, L., Lazzara, G., Nacci, A., Nicotra, G., Noto, R., Pettignano,
 661 A., Spinella, C., Riela, S., 2020a. One-pot synthesis of ZnO nanoparticles supported on halloysite
 662 nanotubes for catalytic applications. *Appl. Clay Sci.* 189.
 663 Massaro, M., Cavallaro, G., Colletti, C.G., D'Azzo, G., Guernelli, S., Lazzara, G., Pieraccini, S.,
 664 Riela, S., 2018a. Halloysite nanotubes for efficient loading, stabilization and controlled release of
 665 insulin. *J. Colloid Interface Sci.* 524, 156-164.
 666 Massaro, M., Colletti, C.G., Guernelli, S., Lazzara, G., Liu, M., Nicotra, G., Noto, R., Parisi, F.,
 667 Pibiri, I., Spinella, C., Riela, S., 2018b. Photoluminescent hybrid nanomaterials from modified
 668 halloysite nanotubes. *J. Mater. Chem. C* 6, 7377-7384.
 669 Massaro, M., Iborra, C.V., Cavallaro, G., Colletti, C.G., García-villén, F., Lazzara, G., Riela, S.,
 670 2021b. Synthesis and characterization of nanomaterial based on halloysite and hectorite clay
 671 minerals covalently bridged. *Nanomaterials* 11, 1-13.
 672 Massaro, M., Noto, R., Riela, S., 2020b. Past, present and future perspectives on halloysite clay
 673 minerals. *Molecules* 25.
 674 Massaro, M., Poma, P., Colletti, C.G., Barattucci, A., Bonaccorsi, P.M., Lazzara, G., Nicotra, G.,
 675 Parisi, F., Salerno, T.M.G., Spinella, C., Riela, S., 2020c. Chemical and biological evaluation of
 676 cross-linked halloysite-curcumin derivatives. *Appl. Clay Sci.* 184.
 677 Massaro, M., Riela, S., Cavallaro, G., Colletti, C.G., Milioto, S., Noto, R., Lazzara, G., 2016.
 678 Ecocompatible Halloysite/Cucurbit[8]uril Hybrid as Efficient Nanosponge for Pollutants
 679 Removal. *ChemistrySelect* 1, 1773-1779.
 680 Naumenko, E.A., Guryanov, I.D., Yendluri, R., Lvov, Y.M., Fakhrullin, R.F., 2016. Clay
 681 nanotube–biopolymer composite scaffolds for tissue engineering. *Nanoscale* 8, 7257-7271.
 682 Peixoto, D., Pereira, I., Pereira-Silva, M., Veiga, F., Hamblin, M.R., Lvov, Y., Liu, M., Paiva-
 683 Santos, A.C., 2021. Emerging role of nanoclays in cancer research, diagnosis, and therapy. *Coord.*
 684 *Chem. Rev.* 440, 213956.
 685 Prishchenko, D.A., Zenkov, E.V., Mazurenko, V.V., Fakhrullin, R.F., Lvov, Y.M., Mazurenko,
 686 V.G., 2018. Molecular dynamics of the halloysite nanotubes. *PCCP* 20, 5841-5849.
 687 Riela, S., Barattucci, A., Barreca, D., Campagna, S., Cavallaro, G., Lazzara, G., Massaro, M.,
 688 Pizzolanti, G., Salerno, T.M.G., Bonaccorsi, P., Puntoriero, F., 2021. Boosting the properties of a
 689 fluorescent dye by encapsulation into halloysite nanotubes. *Dyes Pigm.* 187.
 690 Rozhina, E., Batasheva, S., Miftakhova, R., Yan, X., Vikulina, A., Volodkin, D., Fakhrullin, R.,
 691 2021. Comparative cytotoxicity of kaolinite, halloysite, multiwalled carbon nanotubes and
 692 graphene oxide. *Appl. Clay Sci.* 205, 106041.
 693 Rozhina, E., Panchal, A., Akhatova, F., Lvov, Y., Fakhrullin, R., 2020. Cytocompatibility and
 694 cellular uptake of alkylsilane-modified hydrophobic halloysite nanotubes. *Appl. Clay Sci.* 185,
 695 105371.
 696 Salaa, F., Bendenia, S., Lecomte-Nana, G.L., Khelifa, A., 2020. Enhanced removal of diclofenac
 697 by an organohalloysite intercalated via a novel route: Performance and mechanism. *Chem. Eng. J.*
 698 396.
 699 Sandri, G., Faccendini, A., Longo, M., Ruggeri, M., Rossi, S., Bonferoni, M.C., Miele, D., Prina-
 700 Mello, A., Aguzzi, C., Viseras, C., Ferrari, F., 2020. Halloysite- and Montmorillonite-Loaded
 701 Scaffolds as Enhancers of Chronic Wound Healing. *Pharmaceutics* 12, 179.

Santos, A.C., Pereira, I., Reis, S., Veiga, F., Saleh, M., Lvov, Y., 2019. Biomedical potential of clay nanotube formulations and their toxicity assessment. *Expert Opin. Drug Del.* 16, 1169-1182.

Sharifzadeh, G., Hezaveh, H., Muhamad, I.I., Hashim, S., Khairuddin, N., 2020. Montmorillonite-based polyacrylamide hydrogel rings for controlled vaginal drug delivery. *Mater. Sci. Eng. C* 110, 110609.

Shi, R., Niu, Y., Gong, M., Ye, J., Tian, W., Zhang, L., 2018. Antimicrobial gelatin-based elastomer nanocomposite membrane loaded with ciprofloxacin and polymyxin B sulfate in halloysite nanotubes for wound dressing. *Mater. Sci. Eng. C* 87, 128-138.

Silva, D.T.C., Fonseca, M.G., Borrego-Sánchez, A., Soares, M.F.R., Viseras, C., Sainz-Díaz, C.I., Soares- Sobrinho, J.L., 2020. Adsorption of tamoxifen on montmorillonite surface. *Microporous Mesoporous Mater.* 297, 110012.

Stavitskaya, A.V., Kozlova, E.A., Kurenkova, A.Y., Glotov, A.P., Selischev, D.S., Ivanov, E.V., Kozlov, D.V., Vinokurov, V.A., Fakhrullin, R.F., Lvov, Y.M., 2020. Ru/CdS Quantum Dots Templated on Clay Nanotubes as Visible-Light-Active Photocatalysts: Optimization of S/Cd Ratio and Ru Content. *Chem. Eur. J.* 26, 13085-13092.

Stavitskaya, A.V., Novikov, A.A., Kotelev, M.S., Kopitsyn, D.S., Rozhina, E.V., Ishmukhametov, I.R., Fakhrullin, R.F., Ivanov, E.V., Lvov, Y.M., Vinokurov, V.A., 2018. Fluorescence and Cytotoxicity of Cadmium Sulfide Quantum Dots Stabilized on Clay Nanotubes. *Nanomaterials* 8, 391.

ten Brinke, A.J.W., Bailey, L., Lekkerkerker, H.N.W., Maitland, G.C., 2007. Rheology modification in mixed shape colloidal dispersions. Part I: pure components. *Soft Matter* 3, 1145-1162.

ten Brinke, A.J.W., Bailey, L., Lekkerkerker, H.N.W., Maitland, G.C., 2008. Rheology modification in mixed shape colloidal dispersions. Part II: mixtures. *Soft Matter* 4, 337-348.

Tully, J., Yendluri, R., Lvov, Y., 2016. Halloysite Clay Nanotubes for Enzyme Immobilization. *Biomacromolecules* 17, 615-621.

Turel, I., Bukovec, P., Quirós, M., 1997. Crystal structure of ciprofloxacin hexahydrate and its characterization. *Int. J. Pharm.* 152, 59-65.

Wang, C.-J., Li, Z., Jiang, W.-T., 2011. Adsorption of ciprofloxacin on 2:1 dioctahedral clay minerals. *Appl. Clay Sci.* 53, 723-728.

Williams, L.B., Metge, D.W., Eberl, D.D., Harvey, R.W., Turner, A.G., Prapaipong, P., Poret-Peterson, A.T., 2011. What Makes a Natural Clay Antibacterial? *Environ. Sci. Technol.* 45, 3768-3773.

Wu, Q., Li, Z., Hong, H., Li, R., Jiang, W.-T., 2013. Desorption of ciprofloxacin from clay mineral surfaces. *Water Res.* 47, 259-268.